Development of genetic strategies to treat vision loss in Usher syndrome Type 1C (USH1C)

Dongjoon (Jason) Kim[1], Inga Kristaponyte[1], Bhagwat Alapure[1], Katelyn Robillard[1], Wadih Zein[2], Robert Koenekoop[3], Maria Reinoso[4], and Jennifer J. Lentz[1, 5]

[1] Neuroscience Center of Excellence, LSU Health Sciences Center, New Orleans, LA, USA.
[2] Ophthalmic Genetics and Visual Function Branch, National Eye Institute, National Institutes of Health, Bethesda, MD, USA.
[3] Department of Pediatric Surgery, Montreal Children's Hospital, Montreal, Quebec, Canada.
[4] Department of Ophthalmology, LSU Health Sciences Center, LSU Eye Center, New Orleans, LA, USA.
[5] Department of Otorhinolaryngology, LSU Health Sciences Center, New Orleans, LA, USA.

Introduction

- Usher Syndrome is the leading hereditary cause of combined deaf-blindness in the world[1], characterized by sensorineural hearing loss, night- and peripheral-vision loss through progression of retinitis pigmentosa, and variable onset of vestibular dysfunction[2].
- Usher syndrome is an autosomal recessive disorder categorized into four clinical types (USH1-4) based on age of onset and severity of symptoms, with 15 genes of pathogenic variants currently identified[1, 3].
- Mutations of the *USH1C* gene constitute 6-15% of all USH1 cases[4].
- Specifically, *USH1C c.*216G>A (216A) mutation has been identified as a founder mutation restricted to Acadians in the U.S. and Canada, accounting for nearly all USH1 cases in this population.
- The 216A mutation causes aberrant splicing of the RNA transcript that results in a truncated harmonin protein leading to photoreceptor and hair cell dysfunction[5, 6].
- While the genetic background of *USH1C* is well characterized, treatment options remain limited at this time.
- Antisense oligonucleotides (ASOs) targeting the 216A mutation have been shown to transiently restore hearing, balance, and vision in a mouse model of *USH1C*[7-11].
- Gene replacement therapy via AAV vectors also shows short-term improvements in auditory, vestibular, and visual function[6, 12].
- The *overarching goals* of this project are to extend the duration of therapeutic benefits via CRISPR/Cas9 gene editing of the 216A mutation; and to determine visual outcome measures in USH1C patients that could be used to guide a clinical trial via a prospective natural history study.

Aims of this project:

1. Train in mouse sub-retinal injection techniques to deliver AAV vectors that target photoreceptors.
2. Train in the clinical evaluation of visual function in USH1C patients via a prospective natural history study.

USH1C Genotype & Phenotype

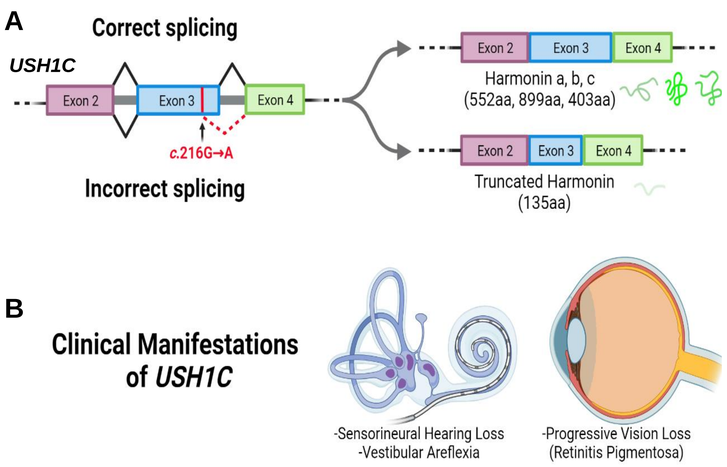

Fig 1. Genetic background of *USH1C c.*216G→A mutation and its clinical manifestations. (**A**) Diagram illustrates gene structure of exons 2-4 of USH1C ("harmonin") and consequences of improper RNA splicing[7]. Normal splicing leads to formation of three possible isotypes of harmonin (harmonin a, b, c) whereas aberrant splicing due to the *c.*216G→A splice site mutation leads to a 35-bp frame-shift deletion of exon 3, producing a truncated form of harmonin protein. Boxes depict exons while lines depict introns. Diagonal lines represent areas of splicing. (**B**) Individuals with *USH1C* exhibit sensorineural hearing loss, which may partially be addressed by cochlear implant at a young age, variable vestibular areflexia, and retinitis pigmentosa with onset at adolescence, leading to progressive loss of visual acuity and visual fields.

Delivery of AAV vectors to mouse retina

Materials and Methods

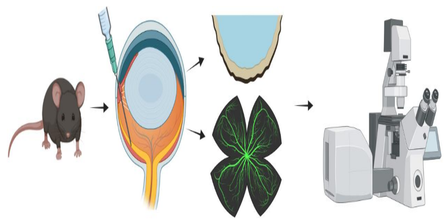

1. One of two AAV vectors (CMV, RK) expressing GFP reporter was injected in the subretinal space through the limbus of USH1C mice.
2. At 2 weeks or 4 weeks post-treatment, retinas were harvested and assessed for viral transduction efficacy via histologic analyses.

Localization of GFP in Retinal Cells

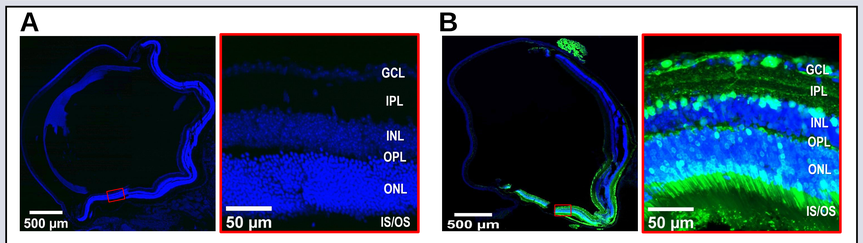

Fig 2. AAV-mediated GFP localization in retinal layers. Images represent transverse retinal cryosections from an (**A**) uninjected control eye and an (**B**) eye subretinally injected with AAV-CMV-GFP. Blue = DAPI; Green = GFP. GCL: ganglion cell layer; IPL: inner plexiform layer; INL: inner nuclear layer; OPL: outer plexiform layer; ONL: outer nuclear layer; IS/OS: photoreceptor inner segments/outer segments. GFP signal was successfully detected in all layers of the retina, including the ONL and IS/OS.

Subretinal Injections of AAV Vectors

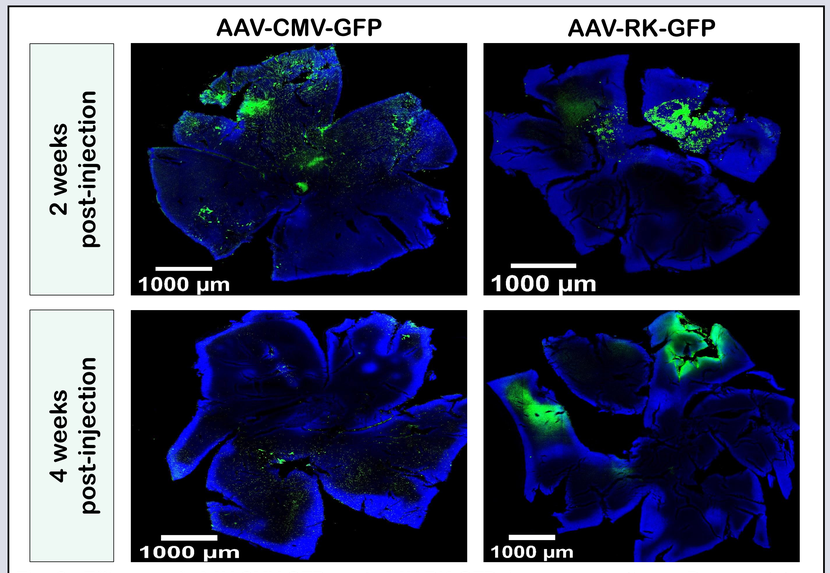

Fig 3. Efficacy of AAV-CMV-GFP and AAV-RK-GFP in mouse retinas. Representative confocal images of retinal whole mounts indicate a single subretinal injection induces AAV-mediated GFP transgene expression in approximately 20-25% of the mouse retina at 2 weeks and 4 weeks post-treatment. The ubiquitous CMV promoter appears to cover more areas of the retina with GFP at 2 weeks post-treatment, but the photoreceptor-specific RK promoter may be more durable long-term at 4 weeks post-treatment. Blue = DAPI; Green = GFP.

Natural History of Vision Loss in USH1C patients

Natural History Study Protocol

1. Patients with genetic confirmation of USH1C disease between the ages of 12 – 70 years are being recruited and their consent collected at 3 clinical sites: MUHC (Montreal, Canada), LSUHSC (New Orleans, LA), and NEI (Bethesda, MD).
2. Patients with concurrent retinal diseases and/or inability to complete the tests are excluded.
3. Patients are being evaluated in six-month intervals over 18 months (4 clinic visits total).
4. Assessments include: ocular history, visual acuity, contrast sensitivity, color vision, visual field, ophthalmic exam, macular integrity, photoreceptor function, funduscopic imaging, optical coherence tomography (OCT), retinal exam, patient reported outcomes via visual functioning questionnaire (VFQ-25).

Progressive Loss of Visual Acuity in USH1C

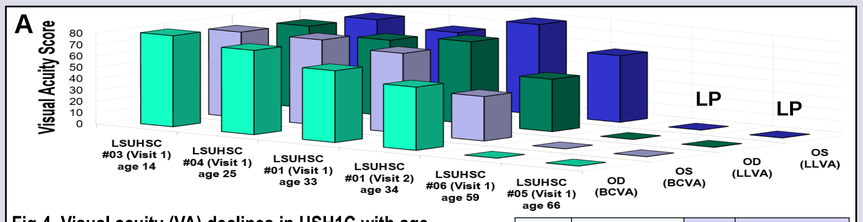

Fig 4. Visual acuity (VA) declines in USH1C with age. (**A**) Best corrected VA (BCVA) and low-luminance VA (LLVA) obtained twice for right (OD) and left (OS) eyes at the clinic visits in 5 USH1C patients using the ETDRS protocol show declining visual acuity with age in USH1C patients. LP: light perception. The VA score increases by 1 point for each letter read correctly on a reading chart, with a maximum of 100%.
(**B**) Average VA scores and their corresponding visual ability. Interestingly, over a 6-month interval in participant #01, average VA score markedly decreased, shifting from normal-moderate loss in VA to a severe loss in VA. OU: both eyes. ICD-9-CM categories indicate levels of visual impairment.

B

	OU AVG (BCVA)	ICD-9-CM Category	OU AVG (LLVA)	ICD-9-CM Category
03 (Visit 1) age 14, F	77.5	Normal	70.75	Moderate Loss
04 (Visit 1) age 25, M	74.5	Normal	65.75	Moderate Loss
01 (Visit 1) age 33, M	66.5	Moderate Loss	75.5	Normal
01 (Visit 2) age 34, M	47.25	Severe Loss	52.25	Severe Loss
06 (Visit 1) age 59, F	0	Near-total Loss	0	Near-total Loss
05 (Visit 1) age 66, F	0	Near-total Loss	0	Near-total Loss

Parafoveal Ring Constriction in USH1C

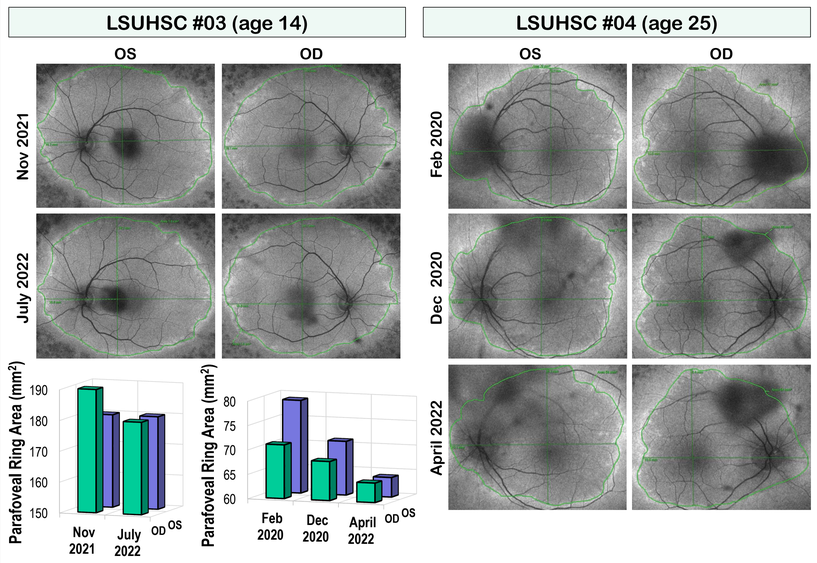

Fig 5. Parafoveal ring of autofluorescence constricts in area over time in USH1C. Representative fundus autofluorescence images from two USH1C patients were taken and areas of the parafoveal ring measured. This ring exemplifies an area of excess photoreceptor phagocytosis, suggestive of photoreceptor degeneration and demarcates the boundary between abnormal peripheral retina and more normal central retina. Parafoveal autofluorescent ring may predict photoreceptor degeneration associated with retinitis pigmentosa and could be used as a diagnostic clinical parameter to assess disease progression.

References

1. Delmaghani S, El-Amraoui A. The genetic and phenotypic landscapes of Usher syndrome: from disease mechanisms to a new classification. *Hum Genet* 2022;141:709-735.
2. Nisenbaum E, Thielhelm TP, Nourbakhsh A, et al. Review of Genotype-Phenotype Correlations in Usher Syndrome. *Ear Hear* 2022;43:1-8.
3. Velde HM, Reurink J, Held S, et al. Usher syndrome type IV: clinically and molecularly confirmed by novel ARSG variants. *Hum Genet* 2022.
4. Koenekoop RK, Arriaga MA, Trzupek KM, Lentz JJ. Usher Syndrome Type I. In: Adam MP, Ardinger HH, Pagon RA, et al. (eds), *GeneReviews((R))*. Seattle (WA); 1993 [updated 2020 Oct 8].
5. Bahloul A, Pepermans E, Raynal B, et al. Conformational switch of harmonin, a submembrane scaffold protein of the hair cell mechanoelectrical transduction machinery. *FEBS Lett* 2017;591:2299-2310.
6. Grotz S, Schafer J, Wunderlich KA, et al. Early disruption of photoreceptor cell architecture and loss of vision in a humanized pig model of usher syndromes. *EMBO Mol Med* 2022;14:e14817.
7. Lentz JJ, Jodelka FM, Hinrich AJ, et al. Rescue of hearing and vestibular function by antisense oligonucleotides in a mouse model of human deafness. *Nat Med* 2013;19:345-350.
8. Lentz JJ, Pan B, Ponnath A, et al. Direct Delivery of Antisense Oligonucleotides to the Middle and Inner Ear Improves Hearing and Balance in Usher Mice. *Mol Ther* 2020;28:2662-2676.
9. Ponnath A, Depreux FF, Jodelka FM, et al. Rescue of Outer Hair Cells with Antisense Oligonucleotides in Usher Mice Is Dependent on Age of Treatment. *J Assoc Res Otolaryngol* 2018;19:1-16.
10. Vijayakumar S, Depreux FF, Jodelka FM, et al. Rescue of peripheral vestibular function in Usher syndrome mice using a splice-switching antisense oligonucleotide. *Hum Mol Genet* 2017;26:3482-3494.
11. Wang L, Kempton JB, Jiang H, et al. Fetal antisense oligonucleotide therapy for congenital deafness and vestibular dysfunction. *Nucleic Acids Res* 2020;48:5065-5080.
12. Pan B, Askew C, Galvin A, et al. Gene therapy restores auditory and vestibular function in a mouse model of Usher syndrome type 1c. *Nat Biotechnol* 2017;35:264-272.

Conclusion

- AAV vectors can be used to safely and effectively transduce retinal cells in mouse eyes.
- Future studies will aim to optimize AAV-mediated delivery of CRISPR/Cas9 gene editing tools (editors) targeting the 216A mutation (guide-RNAs) to treat vision loss associated with USH1C.
- Prospective NHS will continue to expand knowledge on the clinical progression of vision loss in USH1C and help identify potential participants for clinical trials in the future.

Acknowledgments

We gratefully acknowledge support from the National Institutes of Health (R01EY030499), Decibel Therapeutics, Inc., Foundation Fighting Blindness, Ush One See, Usher 2020, and Eye on Jacob Foundations. We would like to thank Dr. Rob Koenekoop at MUHC and Dr. Wadih Zein at NIH/NEI for their helpful comments and assistance on NHS data analysis. We give special thanks to members of the Lentz lab for their invaluable support throughout this project. Graphical diagrams were created using the BioRender software.

This research project was supported through the LSU Health Sciences Center, School of Medicine.